

**Convective Quasi-Equilibrium in Midlatitude Continental
Environment and its Effect on Convective Parameterization**

Guang J. Zhang

Center for Atmospheric Sciences

Scripps Institution of Oceanography

La Jolla CA 92093-0221

Email: gzhang@ucsd.edu

Journal of Geophysical Research, **107(D14)**, 10.1029/2001JD001005.

Abstract

The quasi-equilibrium assumption proposed by Arakawa and Schubert assumes that convection is controlled by the large-scale forcing in a statistical sense, in such a way that the stabilization of the atmosphere by convection is in quasi-equilibrium with the destabilization by the large-scale forcing. The assumption was developed largely based on observations in the tropical maritime environment and has not been evaluated in midlatitudes. This study examines the quasi-equilibrium assumption in midlatitude continental convection environment using summertime observations from the Southern Great Plains of the United States. Two complementary approaches are taken for this purpose. The first one compares the net time rate of change of convective available potential energy to that due to the large-scale forcing. The second one examines the contributions to the net change of CAPE from the boundary layer air and the free tropospheric air above. Results from both the approaches indicate that the quasi-equilibrium assumption is not well suited for midlatitude continental convection. It is shown that the net change of CAPE is comparable to and largely comes from that due to thermodynamic changes of the boundary layer air, while the contribution from the free troposphere above the boundary layer is negligible. The analysis also shows that the role of convective inhibition to suppress convection is the most pronounced when the large-scale forcing in the free troposphere is weak. Based on these and other observations, a modification to the quasi-equilibrium assumption is proposed. It assumes that convective and large-scale processes in the free troposphere above the boundary layer are in balance, so that contribution from the free troposphere to changes in CAPE is negligible. This assumption is then tested using the single column model of the NCAR CCM3 by modifying the closure in the CCM3 convection scheme. Such a modification significantly improves the single column model simulation. The applicability of this new quasi-equilibrium assumption to tropical convection environment is also discussed.

1. Introduction

Convective parameterization is one of the most challenging issues in global climate models (GCM). Convection as represented by convective parameterization schemes in GCMs is controlled by the large-scale dynamic and thermodynamic fields through a closure condition. Such a closure condition is typically determined empirically by the observed relationships between convective activity and the large-scale atmospheric states or processes. Arakawa and Schubert [1974] introduced the concept of quasi-equilibrium between convection and the large-scale forcing. The essence of the quasi-equilibrium assumption is that convection is controlled by the large-scale forcing in a statistical sense, in such a way that the stabilization of the atmosphere by convection is in quasi-equilibrium with the destabilization by the large-scale forcing. This assumption has become the cornerstone in modern convective parameterization development. Most of the convective parameterization schemes nowadays use it one way or another [e. g., Moorthi and Suarez, 1992; Randall and Pan, 1993; Zhang and McFarlane, 1995; Sud and Walker, 2000; Gregory et al., 2000].

In theoretical studies, the quasi-equilibrium assumption has also been used extensively [Emanuel et al., 1994; Neelin, 1997; Yu and Neelin, 1997; Neelin and Zeng, 2000; Zeng et al., 2000] to understand the tropical dynamics and thermodynamics. For example, Neelin and Zeng [2000] constructed a tropical circulation model of intermediate complexity based on the quasi-equilibrium assumption.

The quasi-equilibrium assumption has been examined in a number of observational and numerical studies for tropical convective environment [Arakawa and Schubert, 1974; Arakawa and Chen, 1987; Xu and Arakawa, 1992; Yano et al., 2000]. Arakawa and Schubert [1974] showed, assuming the boundary layer forcing on cloud work function is negligible, that the large-scale forcing in the cloud layer on cloud work function is much larger than the net change of the cloud work function [their Figure 13 and footnote 12]. Yano et al. [2000] examined the asymptotic behavior of the Arakawa and Schubert quasi-equilibrium using an analytic model and output from a cloud-resolving model simulation. Assuming that the sub-cloud layer variables are

time-independent in both their analytic and cloud-resolving models, they showed that the Arakawa-Schubert quasi-equilibrium assumption works well.

On the other hand, it has been known for years that changes in tropospheric mean temperature are minuscule compared to other fields such as diabatic latent heat release and boundary layer equivalent potential temperature in tropical weather systems [Frank, 1980; McBride, 1981; McBride and Frank, 1999]. Frank [1980] showed that during GATE the observed free tropospheric temperature changes are on the order of a few tenths of a degree no matter how large the vertically-integrated diabatic heating and rainfall is. Observations by McBride and Frank [1999] in Australian Monsoon Experiment [AMEX] indicate that the actual stabilization of the atmosphere in response to deep convection occurs almost entirely through the modification of convective available potential energy [CAPE] through decreasing equivalent potential temperature of the source air in the boundary layer. Such observational facts are seldom considered in relation to convective parameterization in general and quasi-equilibrium in particular. The only exception is the work by Fraedrich and McBride [1989] in a theoretical study to understand the physical mechanism of CISK. They parameterized convective heating by assuming a balance between diabatic heating and adiabatic cooling in the free troposphere above the boundary layer such that the net tropospheric temperature change is zero in their two-layer model. With this assumption, they showed that the growth rate of CISK perturbation is independent of the horizontal scale as long as the scale of the disturbance is much smaller than the Rossby deformation radius. This resolved the long-standing problem that perturbations of smallest horizontal scales grow the fastest in classic CISK theory and offered new insight into the physical mechanism of CISK.

Compared to the number of studies for tropical environment, few studies have examined the performance of quasi-equilibrium in midlatitude continental convection. Grell et al. [1991] tested a simplified Arakawa and Schubert scheme for a midlatitude mesoscale convective complex, and found that in such systems, where the large-scale forcing is strong, quasi-equilibrium is a good approximation. But, problems can arise in cases with weak large-scale forcing.

In this study, we examine the applicability of the Arakawa-Schubert convective quasi-equilibrium [hereafter referred to as the AS quasi-equilibrium] in midlatitude continental environment. Section 2 will describe the data and analysis approaches. Section 3 will evaluate the quasi-equilibrium assumption. Based on the results, a modified quasi-equilibrium is proposed in section 4. In section 5, we will test the modified quasi-equilibrium assumption using the Zhang and McFarlane [1995] convection scheme together with the NCAR CCM3 single column model. Section 6 will present the summary and discussions.

2. Data and analysis approach

The data used in this study are from the Southern Great Plains [SGP] site of the Atmospheric Radiation Measurement [ARM] program. Soundings over this area were collected during two Intensive Observation Periods [IOP] in the summers of 1995 and 1997. The summer 1995 IOP covers 16 days from July 18 to Aug. 3, 1995, and the summer 1997 IOP covers 29 days from June 19 to July 18, 1997. The data used to provide the necessary basic meteorological fields include upper-air soundings, wind fields from wind profilers, and the gridded meteorological fields from the NCEP Rapid Update Cycle analysis. The data were processed by Zhang et al. [2001] using variational analysis to provide the large-scale forcing for the single-column model intercomparison projects to test convective parameterization schemes [Ghan et al., 2000; Xie et al. 2001]. The soundings were available at 3-hr intervals. However, the objective

analysis interpolates them to 20-min intervals and provide a single temperature and moisture profile at each time for the entire area representing a GCM grid point. The details of the analysis processes can be found in Zhang et al. [2001]. The large-scale data at the 20-min interval resolution are used in this study to compute the needed fields, such as the time rate of change of CAPE. These fields are then averaged over each 3-hr period to obtain the final results. The vertical resolution of the data is 50 mb starting from 965 mb and ending at 115 mb.

In this study we use CAPE to measure convective instability in the atmosphere. CAPE is defined by:

$$A \equiv CAPE = \int_{p_t}^{p_b} R_d (T_{vp} - T_{ve}) d \ln p \quad (1)$$

Where $T_{vp} = T_p (1 + 0.608 q_p - q_l)$ and $T_{ve} = T_e (1 + 0.608 q_e)$ are the virtual temperatures of the air parcel and its environment as it is lifted from its originating level p_b to the neutral buoyancy level p_t . R_d is the gas constant for dry air. q_l is the liquid water condensed following reversible moist adiabat as the air is lifted. T_e and q_e are the environmental or large-scale temperature and moisture, respectively. T_p and q_p are the parcel's temperature and moisture following a reversible moist adiabat. They are calculated following the method used in Zhang and McFarlane [1991]. For non-entraining parcels, they are entirely determined by the temperature and moisture content at its originating level, which is assumed to be in the boundary layer. For this study, the originating level is set to be the second level from the bottom. It is well known that CAPE values are sensitive to the choice of the parcel's originating level [Emanuel, 1994]. We tested this sensitivity by setting the parcel's originating level to the lowest level. We find that while CAPE values are considerably larger in this case, the conclusions regarding the quasi-equilibrium do not change.

When an air parcel is lifted, it often has to overcome a layer of negative buoyancy immediately above its originating level until the level of free convection. The vertical integral of this negative buoyancy measures the convective inhibition, or CIN:

$$CIN = \int_{p_{lfc}}^{p_b} R_d (T_{vp} - T_{ve}) d \ln p \quad (2)$$

where subscript lfc stands for level of free convection. An air parcel has to have enough lifting power to overcome CIN before convection is possible. Thus, CIN is often viewed as a factor to suppress convection.

The time rate of change of CAPE is given by:

$$\begin{aligned} \frac{\partial A}{\partial t} &= \frac{\partial}{\partial t} \left\{ \int_{p_t}^{p_b} R_d (T_{vp} - T_{ve}) d \ln p \right\} \\ &= \int_{p_t}^{p_b} R_d \left(\frac{\partial T_{vp}}{\partial t} - \frac{\partial T_{ve}}{\partial t} \right) d \ln p - R_d (T_{vp} - T_{ve})_{p=p_t} \frac{\partial p_t}{\partial t} \end{aligned} \quad (3)$$

By definition, at the neutral buoyancy level $T_{vp} = T_{ve}$, thus the last term vanishes in theory. In practice, since finite difference is used for time derivative, the last term occasionally has a small non-zero value when the neutral buoyancy level changes with time. But we will ignore it in our calculation of CAPE change.

Using the convention of Arakawa and Schubert [1974], the net CAPE change can be written as the sum of that due to convective processes (denoted by subscript cu) and that due to large-scale processes (denoted by subscript ls):

$$\frac{\partial A}{\partial t} = \left(\frac{\partial A}{\partial t} \right)_{cu} + \left(\frac{\partial A}{\partial t} \right)_{ls} \quad (4)$$

The AS quasi-equilibrium assumption requires that $\partial A/\partial t \ll (\partial A/\partial t)_{ls}$. Alternatively, noting that [cf. eq. (3)] CAPE change can be expressed in terms of changes in the parcel's and its ambient virtual temperature, eq. (4) can also be rewritten as:

$$\frac{\partial A}{\partial t} = \frac{\partial A_p}{\partial t} + \frac{\partial A_e}{\partial t}, \quad (5)$$

where

$$\frac{\partial A_p}{\partial t} = R_d \int_{p_t}^{p_b} \frac{\partial T_{vp}}{\partial t} d \ln p$$

$$\frac{\partial A_e}{\partial t} = -R_d \int_{p_t}^{p_b} \frac{\partial T_{ve}}{\partial t} d \ln p$$

represent CAPE changes resulting from the parcel's and its ambient virtual temperature changes, respectively. Thus, the quasi-equilibrium assumption requires that $\partial A/\partial t \ll \partial A_p/\partial t$ and $\partial A/\partial t \ll \partial A_e/\partial t$. It is appropriate to point out here that since T_{vp} is entirely determined by boundary layer thermodynamic fields, we will refer to $\partial A_p/\partial t$ as CAPE change due to changes in boundary layer properties. Similarly, since $\partial A_e/\partial t$ measures the vertical integral of the large-scale virtual temperature change from the parcel's originating level to the neutral buoyancy level, we will refer to it as CAPE change due to free tropospheric virtual temperature changes.

In terms of the conventional thermodynamic quantities, we re-write eq. (5) following Emanuel [1994, eqs. (15.3.1) and (15.3.3)]:

$$\frac{\partial A}{\partial t} = C_p (T_{veb} - T_{vet}) \frac{\partial \ln \theta_e}{\partial t} - \frac{\partial}{\partial t} (\phi_t - \phi_b) \quad (5a)$$

where θ_e is the equivalent potential temperature. As before, subscripts b and t stand for a parcel's originating level and the neutral buoyancy level, respectively. ϕ is the geopotential. The first term on the rhs is the net CAPE change due to boundary layer equivalent potential temperature change at the parcel's originating level. The second term is the thickness change of the convection layer. Thus, under quasi-equilibrium, the tropospheric thickness [or mean temperature] and boundary layer entropy change in concert [Emanuel, 1994]. Neelin and Zeng [2000] used this deduction to relate the tropospheric temperature to surface equivalent potential temperature in their tropical circulation model.

As both the parcel's [or boundary layer] and its ambient [or free tropospheric] virtual temperature can change as a result of the large-scale or convective processes, eq. (4) can be formally written as:

$$\frac{\partial A}{\partial t} = \left(\frac{\partial A_p}{\partial t} \right)_{cu} + \left(\frac{\partial A_p}{\partial t} \right)_{ls} + \left(\frac{\partial A_e}{\partial t} \right)_{cu} + \left(\frac{\partial A_e}{\partial t} \right)_{ls} \quad (4a)$$

where

$$\left(\frac{\partial A_p}{\partial t}\right)_{cu} = R_d \int_{p_t}^{p_b} \left(\frac{\partial T_{vp}}{\partial t}\right)_{cu} d \ln p$$

$$\left(\frac{\partial A_p}{\partial t}\right)_{ls} = R_d \int_{p_t}^{p_b} \left(\frac{\partial T_{vp}}{\partial t}\right)_{ls} d \ln p$$

$$\left(\frac{\partial A_e}{\partial t}\right)_{cu} = -R_d \int_{p_t}^{p_b} \left(\frac{\partial T_{ve}}{\partial t}\right)_{cu} d \ln p$$

$$\left(\frac{\partial A_e}{\partial t}\right)_{ls} = -R_d \int_{p_t}^{p_b} \left(\frac{\partial T_{ve}}{\partial t}\right)_{ls} d \ln p$$

On the rhs of eq. (4a), the net CAPE change is broken into four components: CAPE change due to boundary layer virtual temperature change resulting from convective processes $(\partial A_p / \partial t)_{cu}$, CAPE change due to boundary layer virtual temperature change resulting from large-scale processes $(\partial A_p / \partial t)_{ls}$, CAPE change due to free tropospheric virtual temperature change resulting from convective processes $(\partial A_e / \partial t)_{cu}$, and CAPE change due to free tropospheric virtual temperature change resulting from large-scale processes, $(\partial A_e / \partial t)_{ls}$. For example, convection-induced compensatory subsidence warming in the troposphere contributes to $(\partial A_e / \partial t)_{cu}$. Similarly, boundary layer cooling and drying from convective downdrafts contribute to $(\partial A_p / \partial t)_{cu}$. The large-scale advection of temperature and moisture contributes to $(\partial A_e / \partial t)_{ls}$, and the large-scale surface fluxes of heat and moisture contribute to $(\partial A_p / \partial t)_{ls}$. The reason we decompose CAPE change into four components will become clear shortly.

Using ARM observations, we can compute $\partial A / \partial t$ and $(\partial A / \partial t)_{ls}$ as well as their decomposition into the parcel's and the environment's contributions to evaluate the validity of the quasi-equilibrium assumption. $\partial A / \partial t$ is estimated using the observed temperature and moisture profiles. $(\partial A / \partial t)_{ls}$ is estimated using the observed large-scale advection, surface sensible and latent heat fluxes and the radiative cooling from the ECMWF analysis. The CAPE change due to the large-scale forcing is computed as the CAPE difference before and after the forcing is applied to the temperature and moisture fields. To include the effect of surface turbulent fluxes on CAPE change, we assume that the boundary layer is well mixed and that the surface fluxes are linearly distributed over this layer near the surface. Since the boundary layer depth is not known, different values (100 mb and 150 mb) for the layer depth over which surface fluxes are distributed are used for sensitivity tests. For the convenience of presentation, we will use the shorthand dA for CAPE change, a subscript cu or ls for CAPE change resulting from convective or large-scale processes, and a superscript p or e for CAPE changes due to the parcel's or the environment's virtual temperature change. For example, dA_{ls} represents CAPE change resulting from the large-scale processes, and dA_{ls}^e represents CAPE change due to the environmental virtual temperature changes resulting from the large-scale processes.

3. Examination of convective quasi-equilibrium

Fig. 1 shows the time series of CAPE, CIN, the observed precipitation and the CAPE change resulting from the large-scale forcing for the summer 1997 IOP. The x-axis shows days since June 19, 1997. During the IOP the atmosphere in the Southern Great Plains is unstable most of the time, with large values of CAPE. However, convection (as indicated by

precipitation) only occurs episodically. Furthermore, it has little relationship with the amount of CAPE in the atmosphere. The convective inhibition is in general large when there is no convection. More on this will be discussed below.

The large-scale CAPE change due to advection and radiative cooling in the free troposphere, i. e. dA_{ls}^e , coincides well with convection. This observation of the relationship between the two made Xie and Zhang (2000) use the large-scale advective CAPE change as a trigger function for the Zhang and McFarlane (1995) convection scheme. The large-scale CAPE change including the effect of surface turbulent fluxes on boundary layer temperature and moisture is significantly larger most of the time than that without the surface fluxes. The shallower the layer over which the fluxes are distributed, the larger the CAPE changes, because a given amount of heat and moisture fluxes distributed over a shallower boundary layer will have a more pronounced effect on the boundary layer temperature and moisture change. Furthermore, the large-scale CAPE changes including surface fluxes have a strong diurnal cycle due to the diurnal variation in surface fluxes.

In Fig. 1 it is shown that no convection is observed when CIN is large. One explanation is that large CIN poses a strong barrier for air parcels in the boundary layer to be lifted to the level of free convection. Therefore convection is difficult to initiate. To understand its role in suppressing convection, Fig. 2 shows the scatter plot of CIN vs. CAPE and CIN vs. dA_{ls}^e . The data is stratified based on the presence or absence of convection. There is no apparent relationship between convection, CIN and CAPE. Convection can occur under both small and large CIN although the non-convective points are dominant when very large CIN values [larger than 200 J/kg in magnitude] are observed. At a given CAPE value, convection may or may not occur, except for very large CAPE values, where no convection was observed. This is in direct contrast to the assumption that convective activity is proportional to the amount of CAPE in the atmosphere used in CAPE-based convective parameterization schemes.

There is a much clearer separation between convective and non-convective points when CIN is plotted against dA_{ls}^e . When the free tropospheric large-scale forcing is large, convection occurs regardless of the value of CIN. This is probably because the lifting provided by strong large-scale forcing can overcome the negative buoyancy layer below the level of free convection. On the other hand, when CAPE change due to the free tropospheric large-scale forcing is small, convection only occurs when CIN is small, less than 100 J/kg in magnitude. Thus, the role of CIN in suppressing convection is more profound in situations of weak large-scale forcing. It is interesting to note that the maximum CIN in general decreases with the large-scale forcing, likely due to erosion of CIN by sustained large-scale forcing. We also examined a similar plot with dA_{ls}^e replaced by CAPE change including surface fluxes. In this case, the separation between convective and non-convective points seen in Fig. 2b is no longer observed [results not shown], suggesting that the free tropospheric large-scale forcing, but not the total large-scale forcing, is a useful parameter to relate to convection.

Fig. 3 shows the scatter plots of the net CAPE change vs. the CAPE change resulting from the free tropospheric large-scale forcing and the total large-scale forcing including boundary layer processes, i. e., dA vs. dA_{ls}^e and dA vs. dA_{ls} . This type of plot is often used to examine the quasi-equilibrium assumption. The sloping solid line shows the 1:1 ratio for reference. Thus, if the net CAPE change is comparable to CAPE change resulting from the large-scale forcing, the observations should fall along this line. During convective periods, when dA_{ls}^e is large, dA is slightly smaller in magnitude but opposite in sign; when dA_{ls}^e is small, so is dA . On the other hand, during non-convective periods, dA is frequently much larger than dA_{ls}^e ,

suggesting that the free tropospheric large-scale forcing is not responsible for the net CAPE change. When the large-scale forcing, e.g. surface fluxes, on the boundary layer thermodynamic fields is included, the CAPE change due to the total large-scale forcing, i. e., dA_{ls} , is considerably larger than dA_{ls}^e . For fluxes distributed over a 100 mb or 150 mb layer, the qualitative characters are similar. For the quasi-equilibrium assumption to hold, one must have $dA \ll dA_{ls}$, i. e., all the points should fall near the x-axis. However, the figure shows that under convective situation dA is only modestly smaller than dA_{ls} in magnitude. Under non-convective situations, most of the points fall along the 1:1 reference line. Clearly, in these cases the net CAPE change dA is too large for the quasi-equilibrium between convection and the large-scale forcing to hold.

As pointed out earlier in section 2, another way of examining the quasi-equilibrium assumption is to determine if $dA \ll dA^p$ and $dA \ll dA^e$. Fig. 4 shows the time series and the scatter plot of the net CAPE change and CAPE change due to changes in boundary layer temperature and moisture, i. e., dA and dA^p . In addition, it also shows the scatter plot between the net CAPE change and CAPE change due to the free tropospheric virtual temperature change (dA and dA^e). Obviously, dA is very close to dA^p at all times. The scatter plot of dA vs. dA^p shows that in both convective and non-convective situations there is a high degree of correlation [0.98] between the two, with a slope of 0.86. These suggest that most of the net CAPE change results from the boundary layer temperature and moisture changes. On the other hand, CAPE change due to the free tropospheric virtual temperature changes is negligible compared to the net CAPE change, i. e. $dA^e \ll dA$ [Fig. 4c, with a linear regression slope of -0.10]. Recall that the quasi-equilibrium assumption requires that $dA \ll dA^p$ and $dA \ll dA^e$. Fig. 4 clearly shows that the quasi-equilibrium assumption is not valid in midlatitude continental convective environment.

4. A modified quasi-equilibrium assumption

The above analyses show that the net CAPE change is comparable to the CAPE change resulting from the boundary layer thermodynamic changes and is much larger than the CAPE change resulting from the free tropospheric virtual temperature changes. Thus, it is reasonable to assume that CAPE change resulting from the free tropospheric virtual temperature changes is negligible, that is, $dA^e \approx 0$. This is in contrast to the AS quasi-equilibrium. From the viewpoint of CAPE change, the AS quasi-equilibrium assumes that CAPE change resulting from boundary layer thermodynamic changes and that resulting from the free tropospheric virtual temperature changes are in balance, so that the net CAPE change is negligible. On the other hand, here we assume that CAPE change resulting from boundary layer thermodynamic changes and the net CAPE change are in balance, and that CAPE change resulting from the free tropospheric virtual temperature changes is negligible. Mathematically, we can re-write the AS quasi-equilibrium and the modified quasi-equilibrium as:

$$\text{AS quasi-equilibrium:} \quad \frac{\partial A_p}{\partial t} = -\frac{\partial A_e}{\partial t} \quad \Rightarrow \quad \frac{\partial A}{\partial t} \approx 0$$

$$\text{Modified quasi-equilibrium:} \quad \frac{\partial A_p}{\partial t} = \frac{\partial A}{\partial t} \quad \Rightarrow \quad \frac{\partial A_e}{\partial t} \approx 0$$

Similar to the AS quasi-equilibrium concept, dA^e consists of contributions from both convective and large-scale processes,

$$\frac{\partial A_e}{\partial t} = \left(\frac{\partial A_e}{\partial t} \right)_{cu} + \left(\frac{\partial A_e}{\partial t} \right)_{ls}$$

Thus, we assume that a quasi-equilibrium exists between the convective and large-scale modifications of the environmental contribution to CAPE, so that the net contribution (sum of convective and large-scale) is negligible. In terms of tropospheric virtual temperature change, the modified quasi-equilibrium is:

$$\int_{p_t}^{p_b} \frac{\partial T_{ve}}{\partial t} d \ln p = \int_{p_t}^{p_b} \left(\frac{\partial T_{ve}}{\partial t} \right)_{cu} d \ln p + \int_{p_t}^{p_b} \left(\frac{\partial T_{ve}}{\partial t} \right)_{ls} d \ln p \approx 0 \quad (6)$$

In other words, there is a quasi-equilibrium between changes in the tropospheric mean temperature resulting from convective and large-scale processes, such that the net virtual temperature change averaged over the convective layer is negligible [compared to the boundary layer equivalent potential temperature change].

Fig. 5 shows the scatter plot of dA^e vs. dA_{ls}^e . The diagonal line has a 1:1 ratio. All the convective points fall nearly along the x-axis, thus supporting eq. (6). For the non-convective points, dA_{ls}^e is in general small. For these points, the observations are further divided into two groups according to CIN. When CIN is large (< -100 J/kg), many points fall near the 1:1 line for relatively large dA_{ls}^e . This means that for weak, yet non-negligible free tropospheric large-scale forcing, CIN acts to suppress convection. When CIN is small, both dA^e and dA_{ls}^e are small, and the points are clustered around the origin. Comparison of Fig. 5, the modified quasi-equilibrium, with Fig. 3b, the original quasi-equilibrium, demonstrates a clear improvement in relating convection to the large-scale forcing.

Eq. (6) is further tested using an independent dataset from the summer 1995 IOP. Fig. 6 shows the scatter plots of dA vs. dA^p and dA^e vs. dA . For both convective and non-convective periods, the net CAPE change closely follows the CAPE change due to the boundary layer thermodynamic changes, with a slope of 0.89 and a correlation coefficient of 0.98. Similar to Fig. 4c, the CAPE change due to the free tropospheric virtual temperature change is negligible compared to the net CAPE change [dA^e and dA are negatively correlated with a slope of -0.08].

Fig. 7 shows the scatter plots of dA^e vs. dA_{ls}^e and dA vs. dA_{ls} for the summer 1995 IOP. The top frame shows that $dA^e \ll dA_{ls}^e$, again suggesting that the modified quasi-equilibrium proposed in this study works very well. The bottom frame is for the AS quasi-equilibrium assumption. Similar to Fig. 3, it shows that for convective periods, the net CAPE change is somewhat smaller in magnitude than that due to the large-scale forcing. For non-convective periods, the two are comparable, with most of the observations falling along the 1:1 line. Comparison of the two plots shows that without the contamination of the boundary layer forcing on CAPE change, the modified quasi-equilibrium gives a more accurate description of the relationship between convection and the large-scale forcing.

5. Test of the modified quasi-equilibrium in convective parameterization scheme

Similar to the AS quasi-equilibrium assumption, the modified one can also be used as the closure condition for convective parameterization schemes. Here we use the Zhang-McFarlane convection scheme (hereafter referred to as the ZM scheme) and the CCM3 single column model (Hack et al., 1998) to test the assumption proposed in the last section. The closure condition in the original ZM scheme is:

$$M_b = \frac{A}{F\tau} \quad (7)$$

where τ is the time during which CAPE is consumed by convection, and is set to 2 hours in CCM3. F is computed from the thermodynamic profiles and the cloud model. This closure is a variant of the Arakawa Schubert quasi-equilibrium closure, since any deviation of CAPE from

that required by the quasi-equilibrium will be removed at an exponential rate. A similar closure condition has also been proposed by Gregory et al. (2000) in the ECMWF Integrated Forecasting Systems.

On the other hand, the closure condition based on eq. (6) can be written as:

$$\int_{p_i}^{p_b} \left(\frac{\partial T_{ve}}{\partial t} \right)_{cu} d \ln p = \max \left\{ - \int_{p_i}^{p_b} \left(\frac{\partial T_{ve}}{\partial t} \right)_{ls} d \ln p, 0 \right\} \quad (6a)$$

Note that $T_{ve} = T (1 + 0.608q)$ and the effects of convection on temperature and moisture fields in the convection layer are:

$$\left(\frac{\partial T}{\partial t} \right)_{cu} = -M_b \eta \frac{\partial S}{\partial p}$$

$$\left(\frac{\partial q}{\partial t} \right)_{cu} = M_b \left[-\eta \frac{\partial q}{\partial p} + \delta(q_s - q) \right]$$

where M_b is the cloud base mass flux, η is the cloud mass flux at a given level normalized by M_b , and δ is the detrainment of cloud mass flux, also normalized by M_b . q_s is the saturation specific humidity of the detrained cloud air, and S is the large-scale dry static energy. Substituting the above equations into eq. (6a) and rearranging, we have:

$$M_b = \frac{1}{k} \max \left\{ - \int_{p_i}^{p_b} \left(\frac{\partial T_{ve}}{\partial t} \right)_{ls} d \ln p, 0 \right\} \quad (8)$$

where

$$k = \int_{p_i}^{p_b} (1 + 0.608q) \left[-\eta \frac{\partial S}{\partial p} \right] + 0.608T \left[-\eta \frac{\partial q}{\partial p} + \delta(q_s - q) \right] d \ln p.$$

Eq. (8) constitutes the new closure, and the parameterization scheme utilizing it will be referred to as the revised Zhang-McFarlane (RZM) scheme.

In the remainder of this section, we use the large-scale forcing data for the summer 1997 IOP to drive the NCAR CCM3 single column model. Both the closure conditions eq. (7) and eq. (8) are tested. Fig. 8 shows the time series of precipitation from the observations and the model simulations for three convectively active periods. These periods are chosen as they were also the focus periods in an intercomparison project for convective parameterization by the ARM program (Xie et al. 2001). In the first period, there is a weak precipitation event on day 9 and strong precipitation event on day 11. When the original closure is used, the model rains almost daily, with a clear diurnal cycle. This is because CAPE has a strong diurnal cycle due to the surface fluxes. During the strong convection event on day 11, the simulated rainfall is about 65% of the observed. When the new closure is used, both the timing and the intensity of the precipitation events are very well captured. The precipitation events in periods 2 and 3 are less intense. But again, the simulated rainfall using the original closure shows clear diurnal cycle, and the new closure shows noticeable improvement in the rainfall simulation.

Fig. 9 shows the time-height cross section of the temperature biases for the simulations with the original and the new closure. For all three periods, the simulations with the original closure show large warm bias, in the range of 5 to 10 K, relative to the observed temperature fields. The warm biases start to develop early on during each period, and persist throughout the periods. The simulations with the new closure show significantly less temperature bias, most of the time less than 2.5 K in magnitude. In general, there is a slight cold bias in the mid-troposphere. The moisture bias fields [Fig. 10] show similar degree of improvement using the

new closure. There is a large dry bias, 5 to 10 g/kg, between 900 mb and 750 mb in all three convective periods when the original closure is used. This dry bias, together with the warm bias in Fig. 9, may be attributed to the too frequent convection using CAPE-based closure. The new closure largely removes the dry bias, with a tendency to moisten the layer below 800 mb somewhat too much, particularly in the last convective period.

In summary, we showed that for the summer 1997 IOP focussing on midlatitude continental convection, the modified quasi-equilibrium closure makes significant improvement on the simulation of precipitation, temperature and moisture fields. By excluding the CAPE changes associated with the strong boundary layer forcing typically observed on land, the new closure relates convection more realistically to the large-scale forcing.

6. Summary and discussions

This study analyzed the temperature and moisture data from the summers of 1995 and 1997 IOPs for summertime midlatitude continental convection. Two complementary methods are used to examine the convective quasi-equilibrium. It is shown that in such an environment the large-scale forcing and convection are not in the quasi-equilibrium as defined in Arakawa and Schubert [1974]. The net CAPE change, instead of being negligible as required by the AS quasi-equilibrium, represents a major portion [90%] of the CAPE change associated with changes in the boundary layer thermodynamic properties. The contribution to the net CAPE change from the tropospheric temperature and moisture changes is insignificant in magnitude [10% or less] compared to the net CAPE change.

Based on these observations, we proposed a modified quasi-equilibrium between convection and the large-scale forcing. In physical terms, the essence of this modified quasi-equilibrium assumption is that the mean virtual temperature changes in the free troposphere due to convection and the large-scale processes are in quasi-equilibrium, such that its net change is negligible compared to the boundary layer equivalent potential temperature change. This is in contrast to the Arakawa and Schubert quasi-equilibrium assumption that the mean tropospheric virtual temperature and the boundary layer equivalent potential temperature change in concert. The main difference between the modified quasi-equilibrium assumption and the original Arakawa and Schubert quasi-equilibrium assumption lies in the exclusion of the CAPE changes resulting from changes of the boundary layer thermodynamic properties. It is also shown that the effect of convective inhibition on suppressing convection is the most pronounced when the free tropospheric large-scale forcing is weak.

We modified the closure condition of the Zhang and McFarlane convection scheme based on the new quasi-equilibrium assumption, and tested it using the single column version of CCM3 for the summer 1997 IOP. The model simulates the observed precipitation very well. In addition, the temperature and moisture biases in the simulations are significantly reduced compared to the simulations using the original closure. While the single-column model results are encouraging, a true test would be in GCMs. This will be our future work.

In the new closure the boundary layer forcing does not appear directly. However, this does not mean it is not important in convective parameterization. Cooling and drying in the boundary layer due to convective downdrafts can suppress subsequent convection. This is reflected in the convective parameterization through the following facts. First, the atmosphere must be convectively unstable in order for convective parameterization to be activated. Thus, boundary layer forcing including the effect of convective downdrafts has a clear impact on it. Second, boundary layer forcing also affects the amount of convective inhibition. When the free tropospheric forcing is weak, large CIN will act to suppress convection.

Although the new quasi-equilibrium closure is developed from midlatitude data, it has no obvious dependence on midlatitude dynamics, such as large-scale baroclinicity, rotational effects, etc. Rather, the key points hinge on the role of the planetary boundary layer. Furthermore, the essence of the new closure, that is, the net tropospheric mean temperature change is negligible compared to changes in equivalent potential temperature of the boundary layer air, was well observed in the tropical atmosphere [Frank, 1980; McBride and Frank, 1999]. Thus, it is likely that the new closure should also work for tropical convection.

It is interesting to note that although the modified quasi-equilibrium is proposed in this study, its theoretical aspects have already been examined by Yano et al. [2000]. In an attempt to understand the asymptotic behavior of the Arakawa and Schubert quasi-equilibrium, they assumed that the sub-cloud layer variables are time-independent in their linear model. Therefore, the variation of their potential temperature perturbation, or equivalently CAPE, is entirely caused by the large-scale forcing or convective heating above the boundary layer. Thus, the quasi-equilibrium reached in their analytic model was between convection and the large-scale processes in the free troposphere, the same as proposed in this study based on the observations. In addition, in their analysis of the cloud resolving model results for GATE convection, surface fluxes are excluded in their calculation of the large-scale forcing. Again, strictly speaking, their conclusions are applicable to the modified quasi-equilibrium proposed here.

The Arakawa and Schubert quasi-equilibrium was first tested by Grell et al. (1991) in midlatitude mesoscale convective systems. They showed that in such an environment where the large-scale forcing is strong, the Arakawa and Schubert quasi-equilibrium is a good approximation. This is not inconsistent with our results. In the environment of strong convective systems, such as that on day 11 (June 30, 1997), when the GOES satellite imagery shows a strong mesoscale convective system, the net CAPE change is relatively small compared to the large-scale forcing. Thus, the AS quasi-equilibrium is approximately valid. The modified quasi-equilibrium assumption is also consistent with earlier observations. Zhang and McFarlane (1991) showed that the main changes of temperature and moisture in midlatitude convective systems from pre-convection to post-convection occur in the boundary layer while changes in the rest of the troposphere are relatively small.

Georgi and Shields (1999) and Dai et al. (1999) examined the effect of convective parameterization on the precipitation simulation over the continental United States in the NCAR regional climate model. They tested the convective parameterization schemes of Grell (1993), Kuo (1974) and Zhang and McFarlane (1995), and showed that the simulated summer precipitation with all three convection schemes had deficiencies in capturing the pattern of the diurnal cycle of precipitation. The model overestimated precipitation frequency and underestimated precipitation intensity. In particular, convection from the Zhang and McFarlane scheme was overactive. Xie and Zhang (2000) found similar results when they used the Zhang and McFarlane (1995) convection scheme to simulate the precipitation time series in the SGP site of the ARM program with a single column model. To overcome this deficiency, they used the large-scale advective forcing on temperature and moisture as a trigger function. Convection was allowed only when there was large-scale destabilization by the advective forcing, with the amount of convection still determined by the closure of the Zhang and McFarlane scheme. In this study, we take a further step to use the large-scale tropospheric forcing to determine not only the timing, but also the amount of convection.

Another way to remedy overactive convection in models is to impose a relative humidity (RH) threshold for the boundary layer air as a trigger function within the framework of the AS

quasi-equilibrium. In fact, in various implementations of the Arakawa and Schubert (1974) convective parameterization, this is exactly what has been done (Slingo et al., 1996, Sud and Walker, 2000, Wang and Schlesinger 1999). For example, Sud and Walker (2000) required that the boundary layer RH exceed 90% before convection is allowed in their Relaxed Arakawa-Schubert scheme. Wang and Schlesinger (1999) showed that the simulated tropical intraseasonal oscillation strongly depends on the choice of the RH threshold: the higher the threshold, the stronger the simulated intraseasonal oscillation. Arakawa and Cheng (1987) related the boundary layer RH to the AS quasi-equilibrium. They showed that under the quasi-equilibrium condition, the near surface RH is negatively correlated with the lower tropospheric moist temperature lapse rate. Fig. 11 shows such an idealized relationship following Arakawa and Cheng (1987). Here Γ and Γ_m are the average atmospheric lapse rate and the saturation moist adiabatic lapse rate, respectively, in the lower troposphere below 500 mb. The solid line was obtained with $\Gamma=6.5$ K/km and a surface temperature of 296.6 K, both of which are very close to the 29-day mean of the 1997 IOP. The dots are from the summer 1997 IOP observations. If the atmosphere is in the AS quasi-equilibrium, the observations should cluster along the solid line. Consistent with the results in section 3, the observations do not show a significant negative correlation between RH and $\Gamma - \Gamma_m$. It is also seen that the observed near surface RH spans a large range. By imposing a relatively high RH threshold for convection, one only allows a small fraction of what would have been considered as being in convective quasi-equilibrium to be actually so. This in effect confines convection to a small subset of the observations, thereby reducing the frequency of parameterized convection. Therefore, introduction of RH threshold in the Arakawa-Schubert type of convective parameterization has more implications than just a simple convection trigger switch.

Acknowledgments: This research was supported by the Environmental Science Division of U. S. Department of Energy under grant DEFG 0391 ER 61198. The 1997 ARM SGP IOP data used to force the single column model was provided by Dr. S.-C. Xie of Lawrence Livermore National Laboratory. The author thanks Dr. Mitch Moncrieff and an anonymous reviewer for constructive comments that have helped to improve the paper.

References:

- Arakawa, A., and W. H. Schubert, Interaction of a cumulus cloud ensemble with the large-scale environment. Part I. *J. Atmos. Sci.*, **31**, 674-701, 1974.
- Arakawa, A., and J.-M. Chen, Closure assumptions in the cumulus parameterization problem. *Short- and Medium-Range Numerical Prediction, Collection of Papers at the WMO/IUGG NWP Symp.*, Tokyo, Japan, T. Matsuno, Ed., Meteor. Soc. Japan, 107-131, 1987.
- Dai, A., F. Georgi, and K. E. Trenberth, Observed and model-simulated diurnal cycles of precipitation over the contiguous United States. *J. Geophys. Res.*, **104**, 6377-6402, 1999.
- Emanuel, K. A., Atmospheric convection. Oxford University Press, New York, 580 pp, 1994.
- Emanuel, K. A., J. D. Neelin, and C. S. Bretherton, On large scale circulation in convective atmospheres. *Quart. J. Roy. Meteor. Soc.*, **120**, 1111-1143, 1994.
- Fraedrich, K., and J. L. McBride, The physical mechanism of CISK and the free-ride balance. *J. Atmos. Sci.*, **46**, 2642-2648, 1989.
- Frank, W. M., Modulations of the net tropospheric temperature during GATE. *J. Atmos. Sci.*, **37**, 1056-1064, 1980.
- Georgi, F., and C. Shields, Tests of precipitation parameterizations available in the latest version of NCAR regional climate model (RegCM) over continental United States. *J. Geophys. Res.*, **104**, 6353-6375, 1999.
- Gregory, D., J.-J. Morcrette, C. Jacob, A. C. M. Beljaars, and T. Stockdale, Revision of convection, radiation and cloud schemes in the ECMWF Integrated Forecasting System. *Quart. J. Roy. Meteor. Soc.*, **126**, 1685-1710, 2000.
- Grell, G. A., Kuo, Y.-H., and Pasch, R. J., Semiprognostic tests of cumulus parameterization schemes in the middle latitudes. *Mon. Wea. Rev.*, **119**, 5-30, 1991.
- Hack, J. J., J. A. Pedretti, and J. Petch, SCCM User's Guide. Version 1.1 [Available online at <http://www.cgd.ucar.edu/cms/sccm/sccmug.html>], 1998.
- Kuo, H.-L., Further studies of the parameterization of the influence of cumulus convection on large-scale flow. *J. Atmos. Sci.*, **31**, 1232-1240, 1974.
- McBride, J. L., Observational analysis of tropical cyclone formation. Part III: Budget analysis. *J. Atmos. Sci.*, **38**, 1152-1166, 1981.
- McBride, J. L., and W. M. Frank, Relationship between stability and monsoon convection. *J. Atmos. Sci.*, **56**, 24-36, 1999.
- Moorthi, S., and M. J. Suarez, Relaxed Arakawa-Schubert: A parameterization of moist convection for general circulation models. *Mon. Wea. Rev.*, **120**, 978-1002, 1992.
- Neelin, J. D., Implications of convective quasi-equilibrium for the large-scale flow. *The physics and Parameterization of Moist Atmospheric Convection*. R. K. Smith, Ed., Kluwer Academic Publishers, 413-446, 1997.
- Neelin, J. D., and N. Zeng, A quasi-equilibrium tropical circulation model---- Formulation. *J. Atmos. Sci.*, **57**, 1741-1766, 2000.
- Randall, D. A., and D.-M. Pan, Implementation of the Arakawa-Schubert cumulus parameterization with a prognostic closure. *The Representation of Cumulus Convection in Numerical Models of the Atmosphere*, K. A. Emanuel and D. J. Raymond, Eds. Meteor. Monogr. No. 46, 137-144, 1993.
- Slingo, J. M., K. R. Sperber, J. S. Boyle, and others, Intraseasonal oscillations in 15 atmospheric general circulation models: results from an AMIP diagnostic subproject. *Climate Dyn.* **12**, 325-357, 1996.

- Sud, Y. C., and G. K. Walker, Microphysics of clouds with the Relaxed Arakawa-Schubert Scheme (McRAS). Part I: Design and evaluation with GATE Phase III data. *J. Atmos. Sci.*, **56**, 3196-3220, 2000.
- Wang, W., and M. E. Schlesinger, The dependence of convection parameterization of the tropical intraseasonal oscillation simulated by the UIUC 11-layer atmospheric GCM. *J. Climate*, **12**, 1423-1457, 1999.
- Xie, S.-C., and M.-H. Zhang, Impact of the convective triggering function on single-column model simulations. *J. Geophys. Res.*, **105**, 14983-14996, 2000.
- Xie, S.-C., R. T. Cederwall, K.-M. Xu, and coauthors, Intercomparison and evaluation of GCM cumulus parameterizations under summertime midlatitude continental conditions. Submitted to *Quart. J. Roy. Meteor. Soc.*, 2001.
- Xu, K.-M., and A. Arakawa, Semi-prognostic tests of the Arakawa-Schubert cumulus parameterization using simulated data. *J. Atmos. Sci.*, **49**, 2421-2436, 1992.
- Xu, K.-M., and D. A. Randall, Influence of Large-scale advective cooling and moistening effects on the quasi-equilibrium behavior of explicitly simulated cumulus ensembles. *J. Atmos. Sci.*, **55**, 896-909, 1998.
- Yano, J.-Y., W. W. Grabowski, G. L. Roff, and B. E. Mapes, Asymptotic approaches to convective quasi-equilibrium, *Q. J. R. Meteor. Soc.*, **126**, 1861-1887, 2000.
- Yu, J.-Y., and J. D. Neelin, Analytic approximations for moist convectively adjusted regions. *J. Atmos. Sci.*, **54**, 1054-1063, 1997.
- Zeng, N., J. D. Neelin, and C. Chou, A quasi-equilibrium tropical circulation model---Implementation and simulations. *J. Atmos. Sci.*, **57**, 1767-1796, 2000.
- Zhang, G. J. and N. A. McFarlane, Convective stabilization in midlatitudes. *Mon. Wea. Rev.*, **119**, 1915-1928, 1991.
- Zhang, G. J., and N. A. McFarlane, Sensitivity of climate simulations to the parameterization of cumulus convection in the Canadian Climate Centre general circulation model. *Atmosphere-Ocean*, **33**, 407-446, 1995.
- Zhang, G. J., J. T. Kiehl, and P.J. Rasch, Response of climate simulation to a new convective parameterization in the National Center for Atmospheric Research Community Climate Model (CCM3), *J. Climate*, **11**, 2097-2115, 1998.
- Zhang, M.-H., J. L. Lin, R. T. Cederwall, J. J. Yio, and S.-C. Xie, Objective analysis of ARM IOP data: Method and sensitivity. *Mon. Wea. Rev.*, **129**, 295-311, 2001.

Figure Captions:

- Fig. 1: Time series of observed CAPE, CIN and precipitation (upper panel), and the time series of CAPE change due to the large-scale forcing without surface fluxes (solid), with surface fluxes distributed over the lowest 150 mb (dashed) and 100 mb (dotted), respectively.
- Fig. 2: Scatter plots of (a) CIN vs. CAPE, and (b) CIN vs. CAPE change due to the large-scale forcing without surface fluxes. The pluses are for non-convective periods, and the triangles are convective periods.
- Fig. 3: Scatter plots of the net CAPE change vs. the large-scale forcing (a) without surface fluxes, (b) with surface fluxes distributed over the lowest 150 mb layer, and (c) with surface fluxes distributed over the lowest 100 mb layer.
- Fig. 4: (a) Time series and (b) scatter plot of the net CAPE change and the CAPE change due to parcel's virtual temperature change, (c) scatter plot of CAPE change due to the ambient virtual temperature change vs. the net CAPE change. In (b) and (c) triangles and pluses are for convective and non-convective periods, respectively.
- Fig. 5: Scatter plot of the CAPE change due to the ambient virtual temperature change vs. the CAPE change due to the large-scale forcing from advection and radiative cooling. Triangles are for convective periods, pluses and dots are for non-convective periods, the latter of which are for $CIN < -100$ J/kg.
- Fig. 6: Same as Fig 4b, c except for the summer 1995 IOP.
- Fig. 7: Scatter plots of (a) the CAPE change from the ambient virtual temperature change vs. the CAPE change from the large-scale forcing from advection and radiative cooling, (b) the net CAPE change vs. the CAPE change from the large-scale forcing including surface fluxes. (a) shows the modified quasi-equilibrium while (b) shows the AS quasi-equilibrium.
- Fig. 8: Time series of observed and simulated precipitation for three convectively active periods of the summer 1997 IOP.
- Fig. 9: Time-height cross section of temperature bias (model-observation) for the three convectively active periods shown in Fig. 8. The left panel is with the old closure and the right panel is with the new closure.
- Fig. 10: Same as Fig. 9, except for specific humidity.
- Fig. 11: Idealized relationship between surface relative humidity and $\Gamma - \Gamma_m$ under the AS quasi-equilibrium (solid line). The scatter plot shows the observed near surface RH and $\Gamma - \Gamma_m$ averaged over the lower troposphere for the summer 1997 IOP.

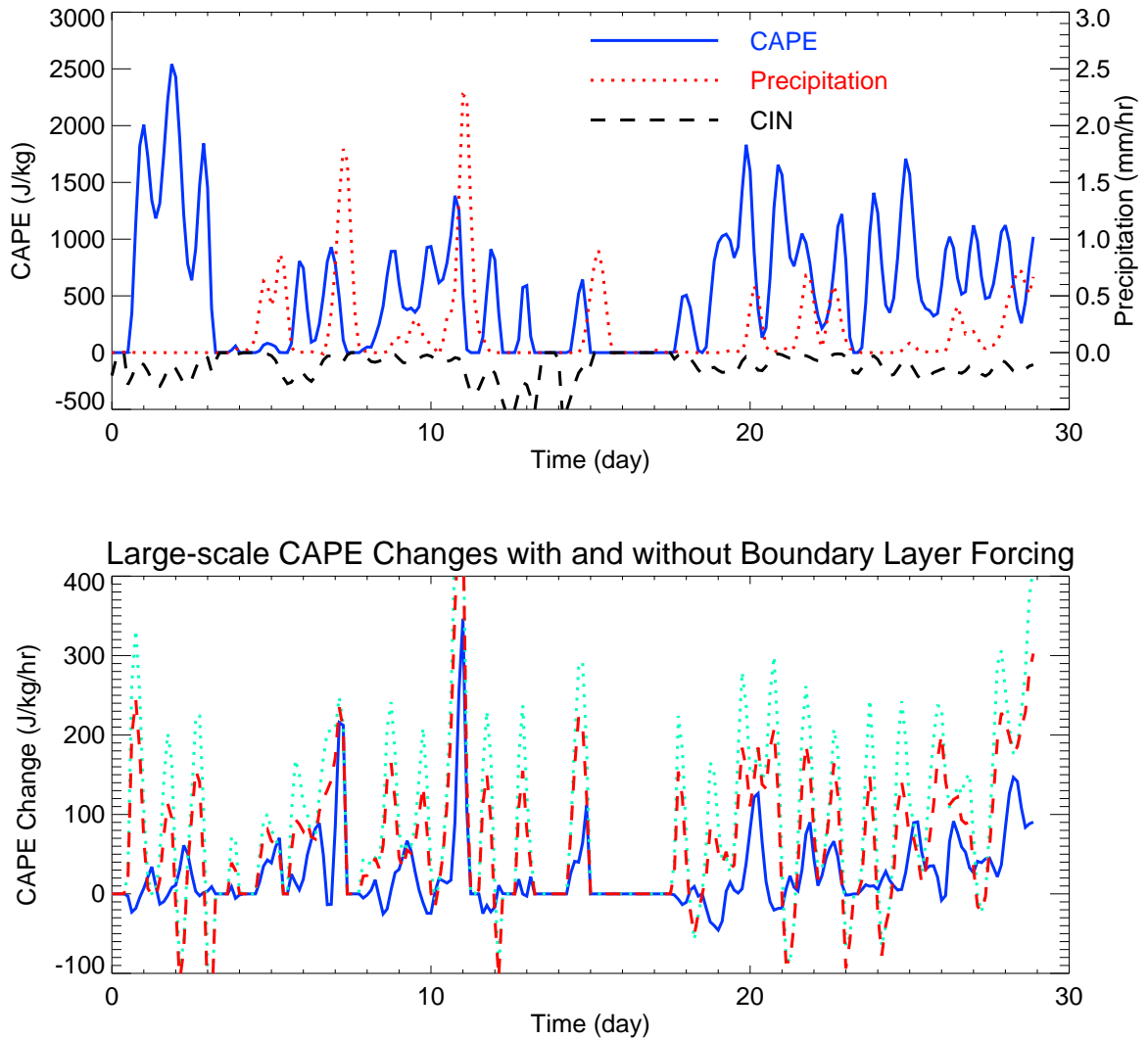


Fig. 1: Time series of observed CAPE, CIN and precipitation (upper panel), and the time series of CAPE change due to the large-scale forcing without surface fluxes (solid), with surface fluxes distributed over the lowest 150 mb (dashed) and 100 mb (dotted), respectively.

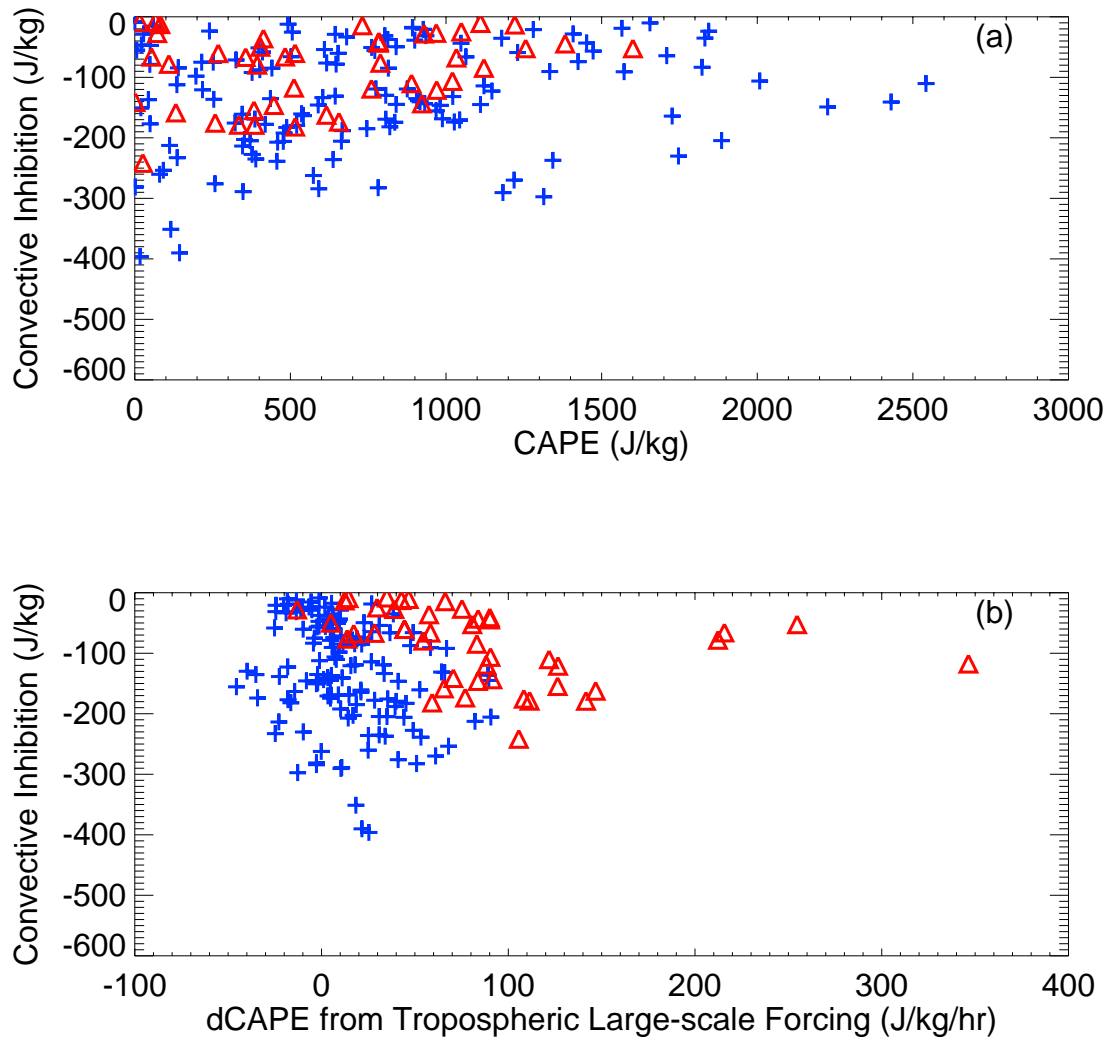


Fig. 2: Scatter plots of (a) CIN vs. CAPE, and (b) CIN vs. CAPE change due to the large-scale forcing without surface fluxes. The pluses are for non-convective periods, and the triangles are convective periods.

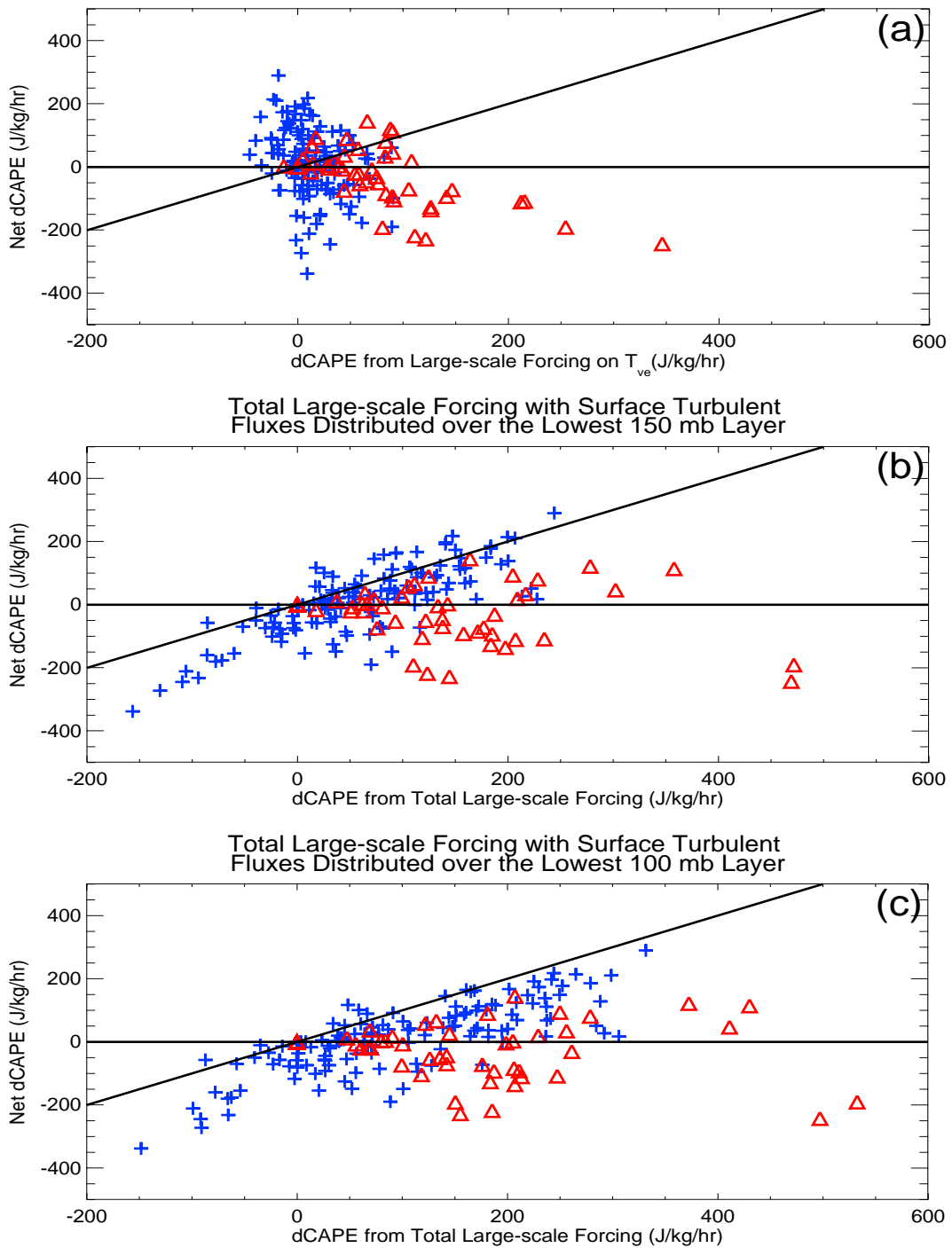


Fig. 3: Scatter plots of the net CAPE change vs. the large-scale forcing (a) without surface fluxes, (b) with surface fluxes distributed over the lowest 150 mb layer, and (c) with surface fluxes distributed over the lowest 100 mb layer.

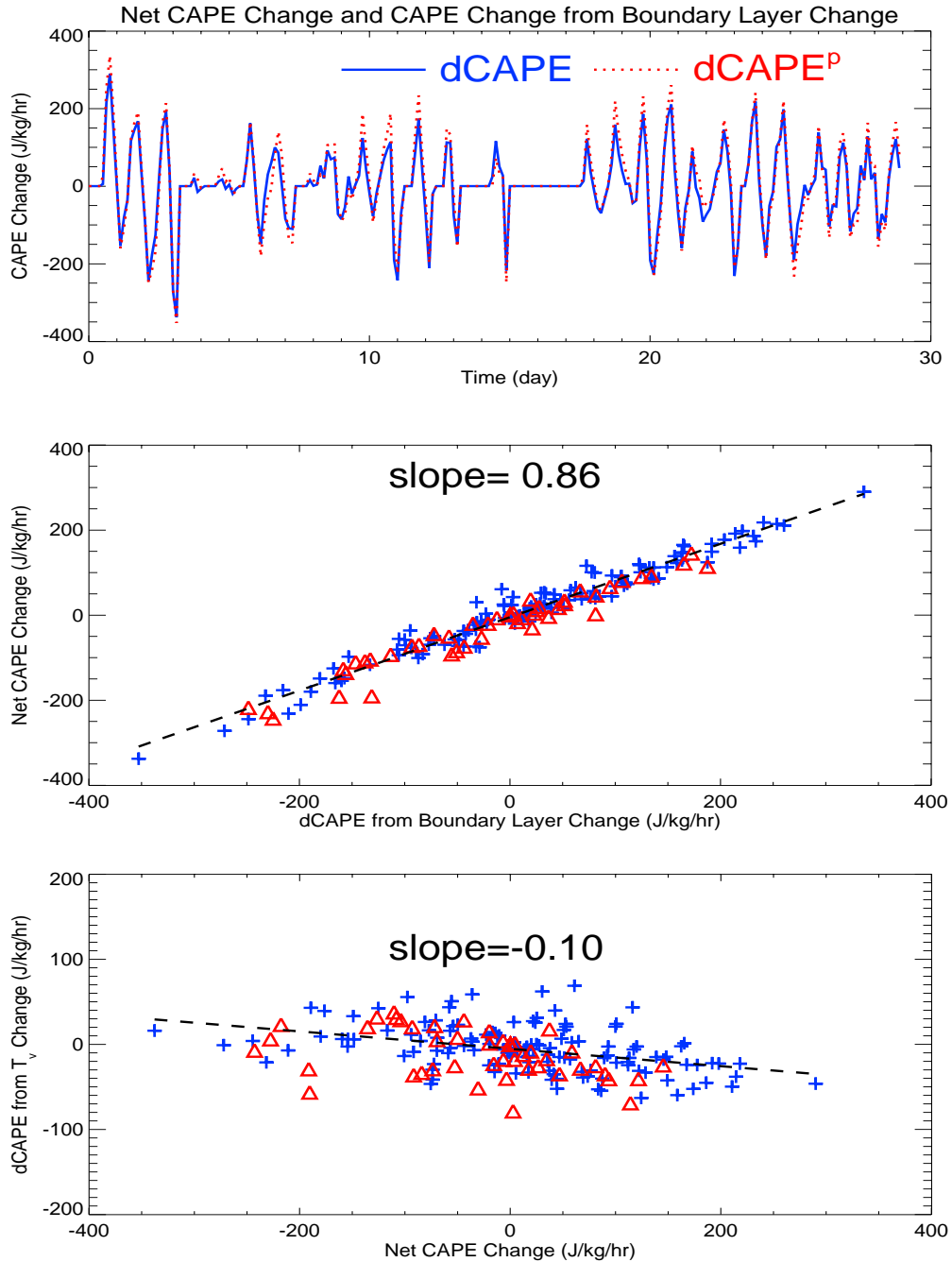


Fig. 4: (a) Time series and (b) scatter plot of the net CAPE change and the CAPE change due to parcel's virtual temperature change, (c) scatter plot of CAPE change due to the ambient virtual temperature change vs. the net CAPE change. In (b) and (c) triangles and pluses are for convective and non-convective periods, respectively.

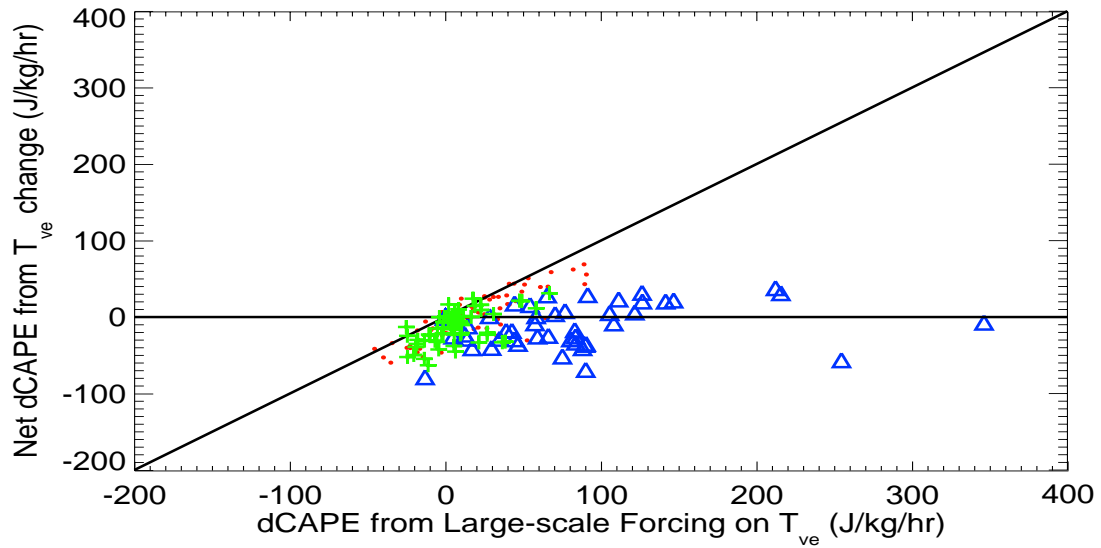


Fig. 5: Scatter plot of the CAPE change due to the ambient virtual temperature change vs. the CAPE change due to the large-scale forcing from advection and radiative cooling. Triangles are for convective periods, pluses and dots are for non-convective periods, the latter of which are for $CIN < -100$ J/kg.

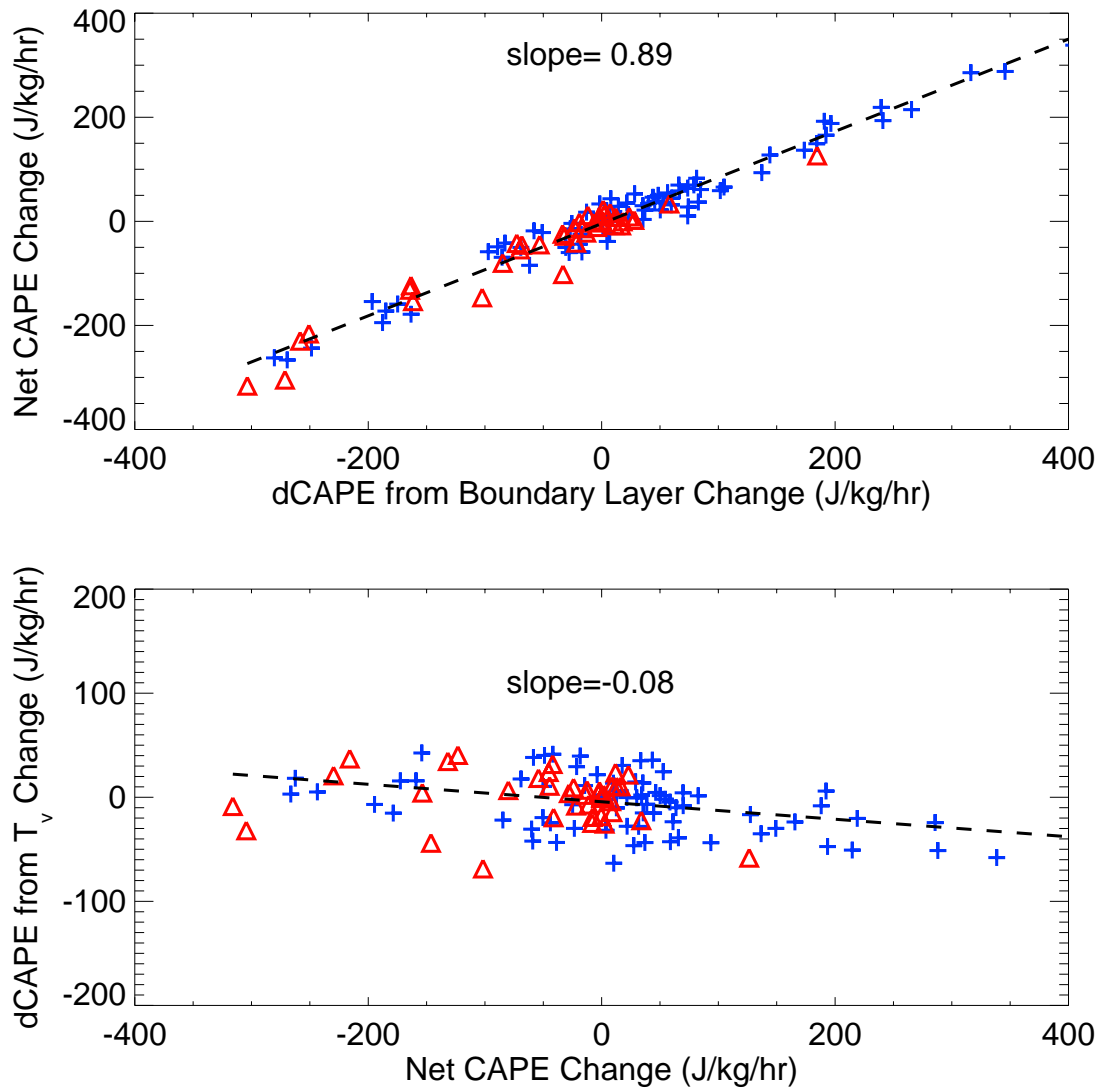


Fig. 6: Same as Fig 4b, c except for the summer 1995 IOP.

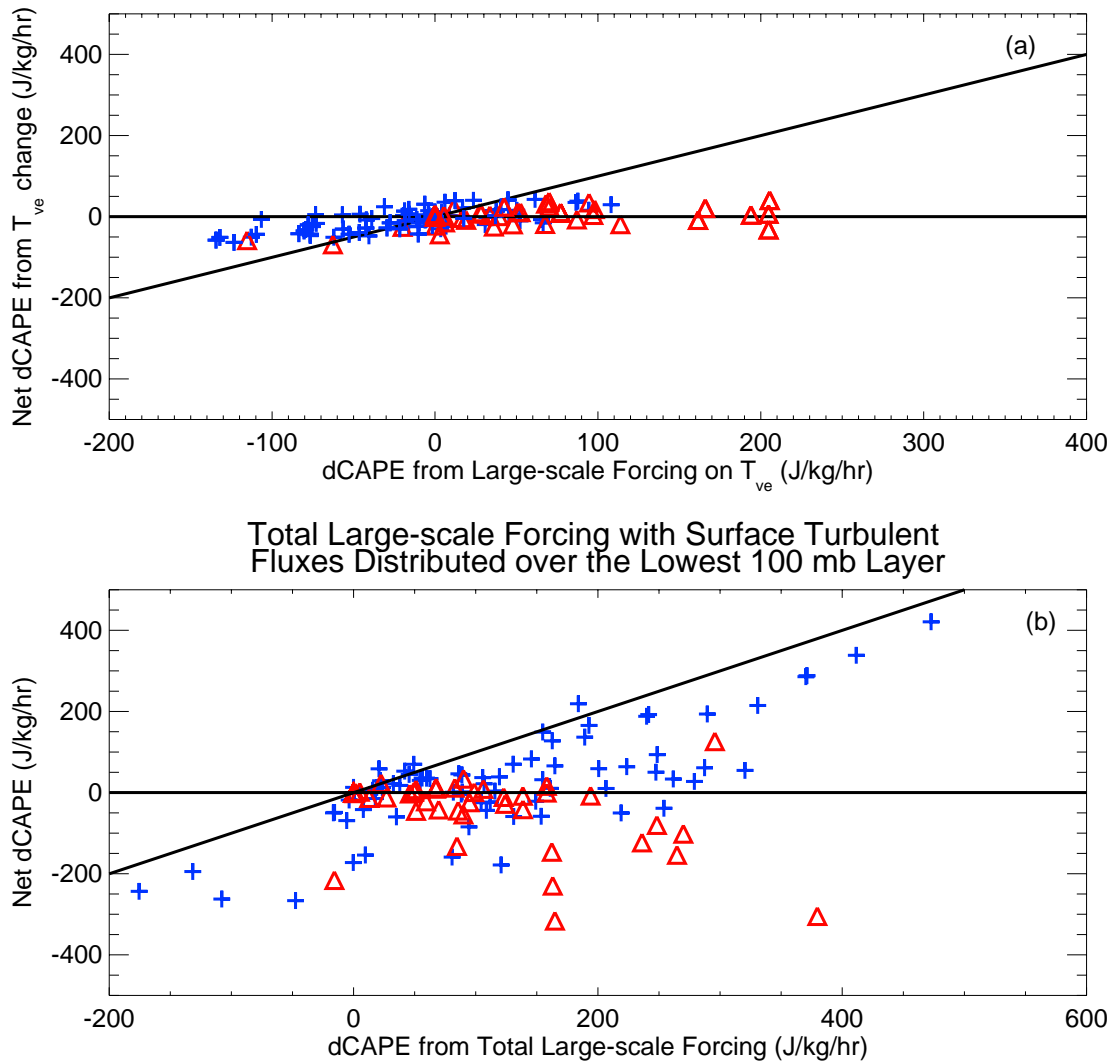


Fig. 7: Scatter plots of (a) the CAPE change from the ambient virtual temperature change vs. the CAPE change from the large-scale forcing from advection and radiative cooling, (b) the net CAPE change vs. the CAPE change from the large-scale forcing including surface fluxes. (a) shows the modified quasi-equilibrium while (b) shows the AS quasi-equilibrium.

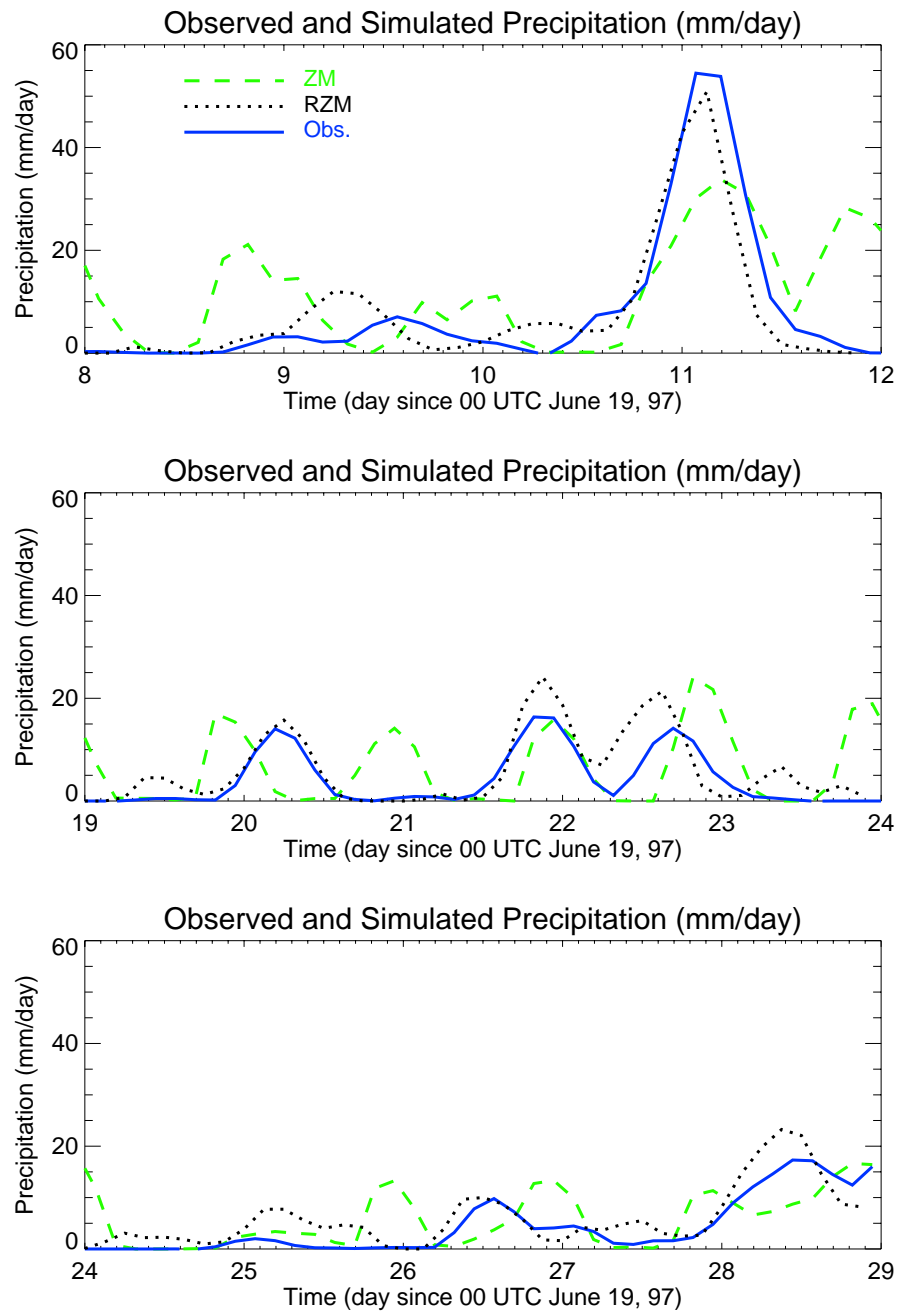


Fig. 8: Time series of observed and simulated precipitation for three convectively active periods of the summer 1997 IOP.

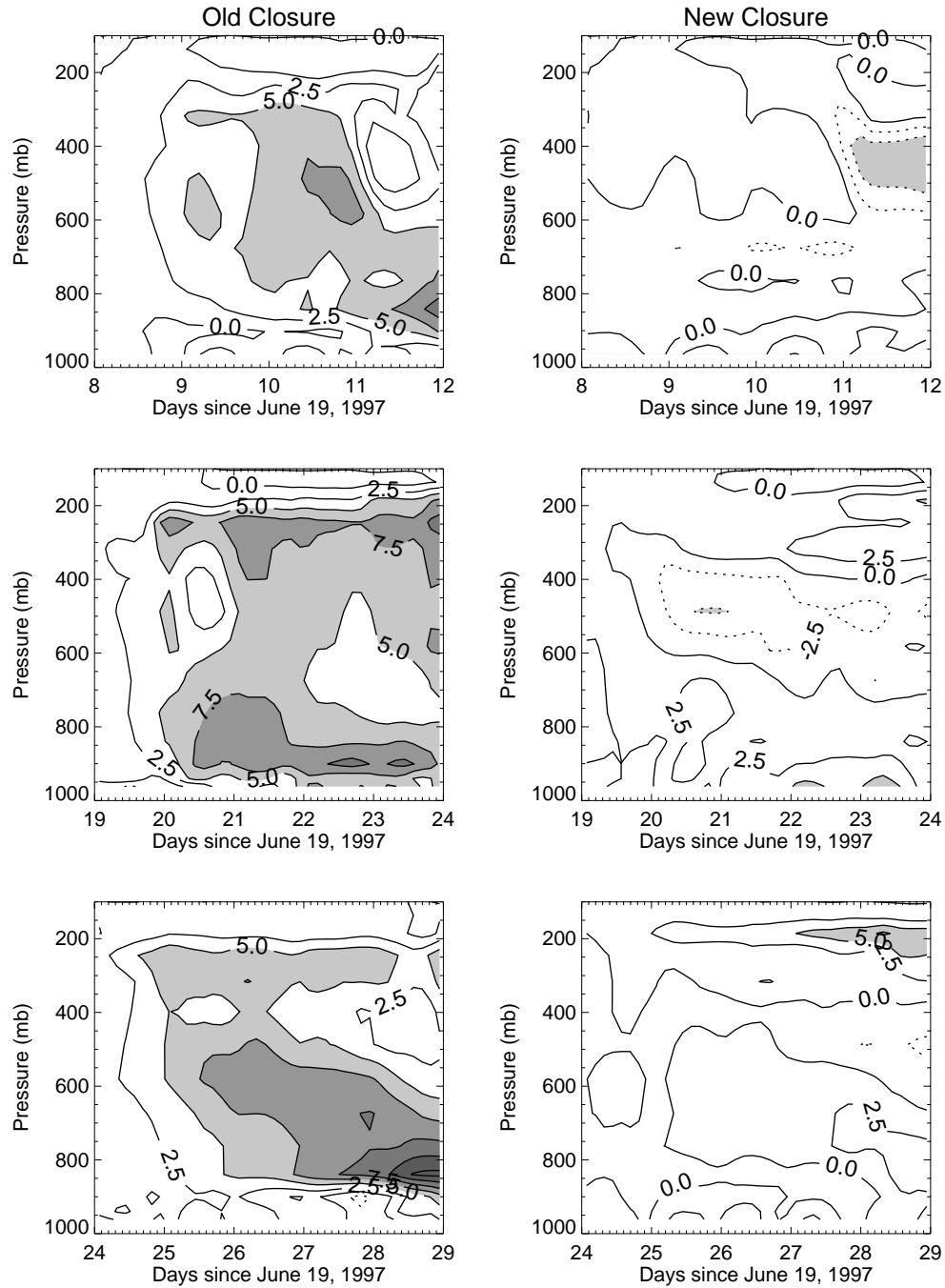


Fig. 9: Time-height cross section of temperature bias (model-observation) for the three convectively active periods shown in Fig. 8. The left panel is with the old closure and the right panel is with the new closure.

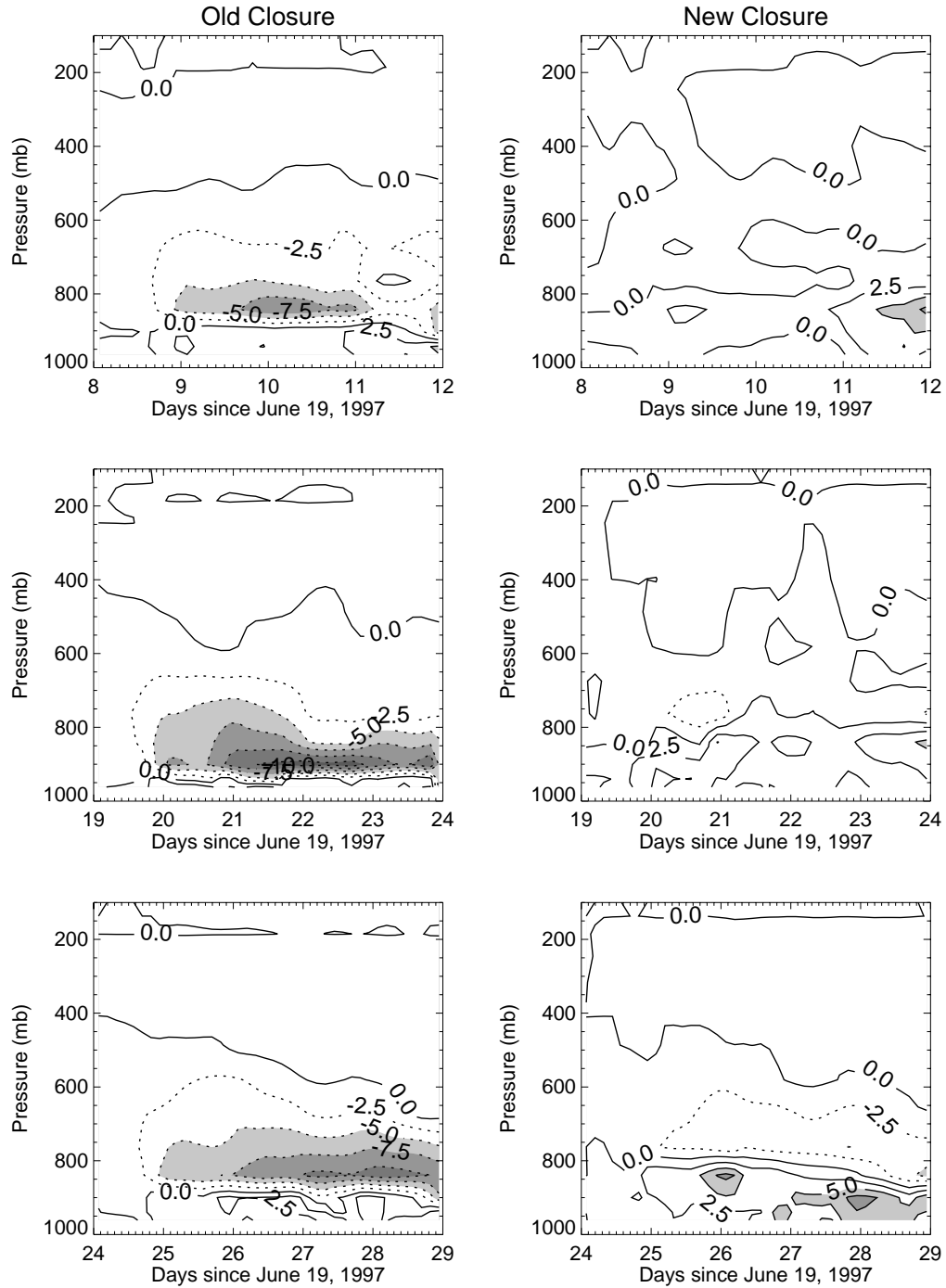


Fig. 10: Same as Fig. 9, except for specific humidity.

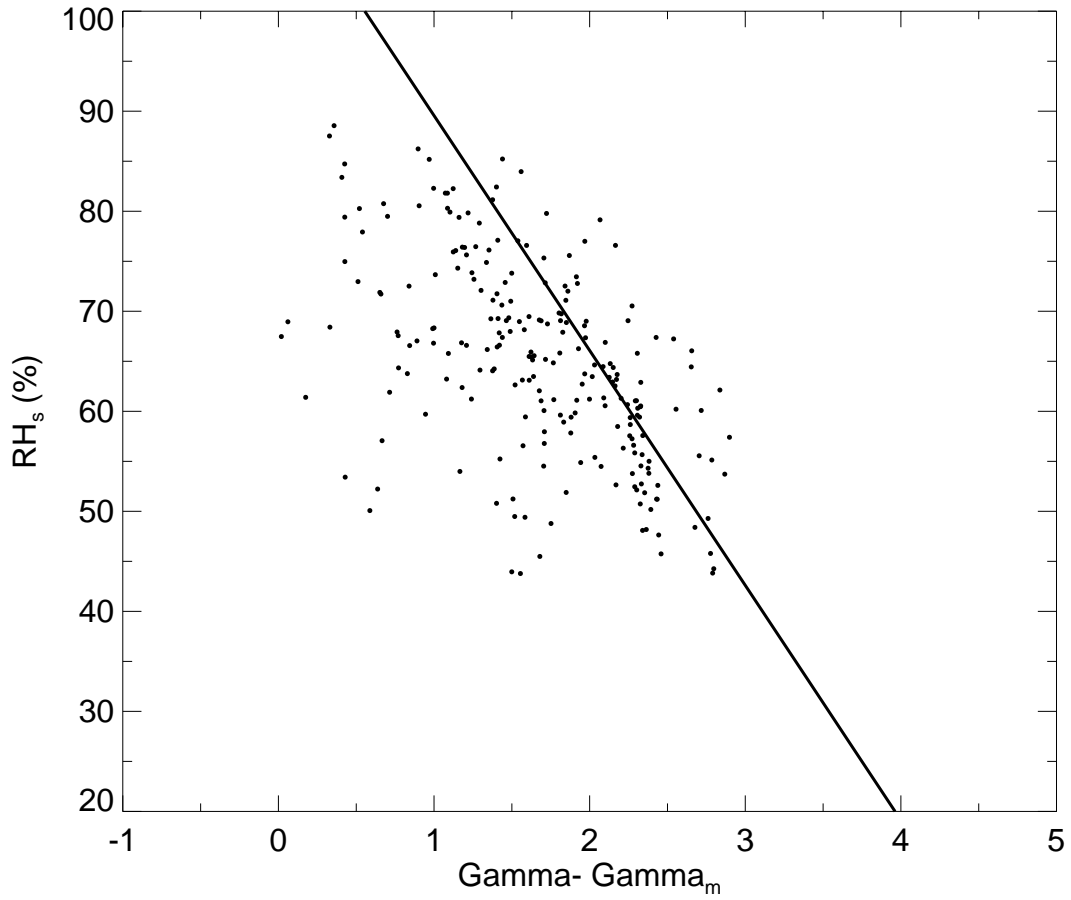


Fig. 11: Idealized relationship between surface relative humidity and $\Gamma - \Gamma_m$ under the AS quasi-equilibrium (solid line). The scatter plot shows the observed near surface RH and $\Gamma - \Gamma_m$ averaged over the lower troposphere for the summer 1997 IOP.